depth. Then we evaluated contributions of different factors on vergence angle by conducting three-factor ANOVA with optic flow, the gaze-area depth, and the movie condition (2D or 3D) as three major factors, and post hoc analyses using the SPSS software (ver.18, SPSS Co. Ltd., USA). Line and curve fitting on the post hoc data was conducted on MATLAB with the Curve-fitting toolbox.

3. Results

We initially tested whether vergence should persist during prolonged 2D random-dot movie presentation in the absence of binocular disparity by measuring eye positions while the subject viewed a radially expanding optic flow (Fig. 1a). We found that the continuous 2D optic flow did elicit sustained vergence reliably across all subjects regardless of whether fixation spot was presented on a screen (red line in Fig. 1b) or not (blue line in Fig. 1b). Following an onset latency, the vergence angle rapidly increased from the initial screen level (θ_0 in Fig. 1a), soon reached a plateau level, and was maintained for at least 30 s throughout the entire stimulation period (Fig 1b). When optic flow stopped, the vergence angle slowly returned to the initial level with some overshoot divergence. It should be noted that vergence eye movements occurred even when the subjects were instructed to gaze at the fixation spot on the screen (red lines in Fig. 1b and c). Vergence time courses were similar irrespective of the fixation condition (see Fig. 1 legend).

Next, we used a video movie showing a passenger's view of a roller coaster as visual stimuli for two purposes. First, we tested if a continuous optic flow fluctuating with the coaster's velocity (Fig. 2a) would elicit persistent vergence eye movements in 2D condition. Second, we examined how the two major depth cues, namely, optic flow and binocular disparity, would interact for the generation of vergence in 3D condition. In 3D condition, two movies with the same content recorded by dual cameras from slightly different views were stereoscopically presented to individual eyes, whereas in 2D condition, the identical video movie was presented to both eyes. We found that the horizontal and vertical gaze positions were not so significantly different between 2D and 3D conditions (Supplementary Fig. 2). This means that subjects gazed at the same area independently of the movie conditions. As predicted by our hypothesis, the 2D video movie induced persistent and dynamical vergence eye movements (Fig. 2b) fluctuating with radial optic flow produced by forward moving scenes. Unexpectedly, not only convergence but also divergence eye movements were elicited in 2D condition, even though the movie included only expanding optic flow components (Fig. 2a). This finding suggests that 2D cues other than optic flow in the movie induced vergence eye movements. A comparison of the time courses of vergence between 2D and 3D conditions (Fig. 2b and c) revealed that the 2D movie induced divergence almost exclusively in the scenes where the 3D movie induced strong divergence. These scenes contained neither optic flow (Fig. 2a) nor binocular disparity in 2D condition; however, they typically contained rich pictorial perspective cues such as forward-extending rail tracks (* or ** in Fig. 2a and e). The subjects significantly perceived depth sensation not only in the 3D movie but also in the 2D movie (Supplementary Fig. 1). Quite interestingly, in the absence of instructions to control the gaze, all the subjects exhibited essentially identical conjugate eye movements for 2D and 3D conditions with little inter-subject variability (Supplementary Fig. 2). These findings raised the possibility that pictorial depth information in a gaze window in 2D condition might be in parallel with binocular disparity information in the gaze window in 3D condition, and the former would be one of the critical determinants of vergence in 2D condition.

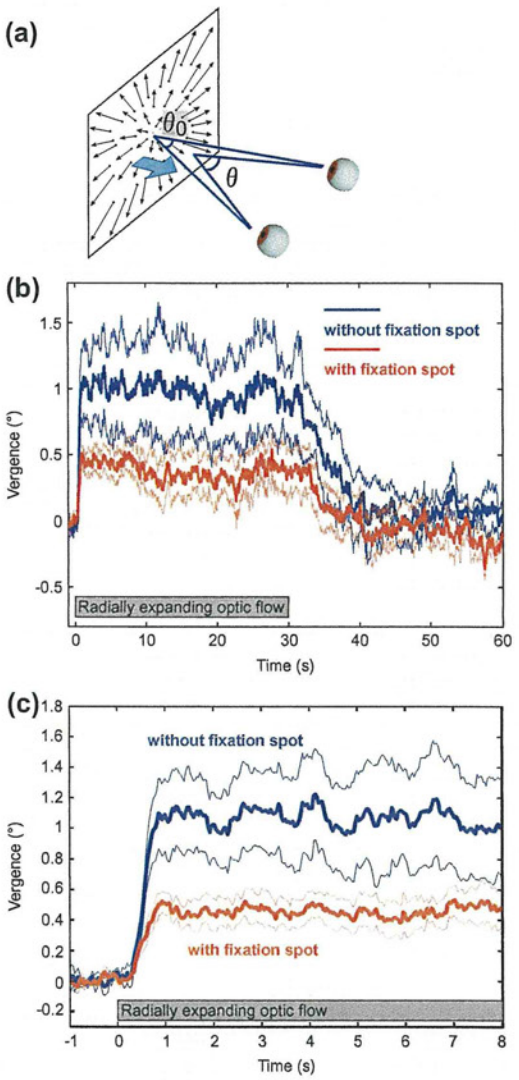

Fig. 1. Sustained vergence elicited by prolonged exposure to an expanding random-dot movie. (a) Radially expanding optic flow defined by moving random-dot movie. As the radial optic flow induces a sensation of forwarding self motion, convergence eye movement (blue arrow) occurs and the vergence angle (θ) increases from the initial screen level (θ_0). (b) Time course of vergence eye movement while the subject viewed a constant-velocity radially expanding optic flow with (red line) or without (blue line) a fixation spot. Thick and thin lines indicate mean ± SEM ($n = 6$). (c) Magnified view of the initial 8-s period from b. The latency with/without the fixation spot was 0.25 ± 0.07 s/0.26 ± 0.05 s, respectively (mean ± SD). The rise and fall time was 0.48 ± 0.14 s/0.52 ± 0.19 s, and 4.34 ± 6.79 s/11.42 ± 7.36 s, respectively, but the plateau-level without the fixation spot (0.97°) was much larger than that with the fixation spot (0.37°). Overshoot vergence was observed after optic flow stopped. The rebound divergence was large and sustained especially in "with fixation spot" condition.

To test this possibility, we defined a 5 × 5° gaze window centered at the gaze point in both 2D and 3D conditions, and estimated "gaze-area depth" for each video frame by averaging the binocular disparity within the gaze window (Fig. 2d and e). Gaze-area depth within a 2D picture was defined as the mean

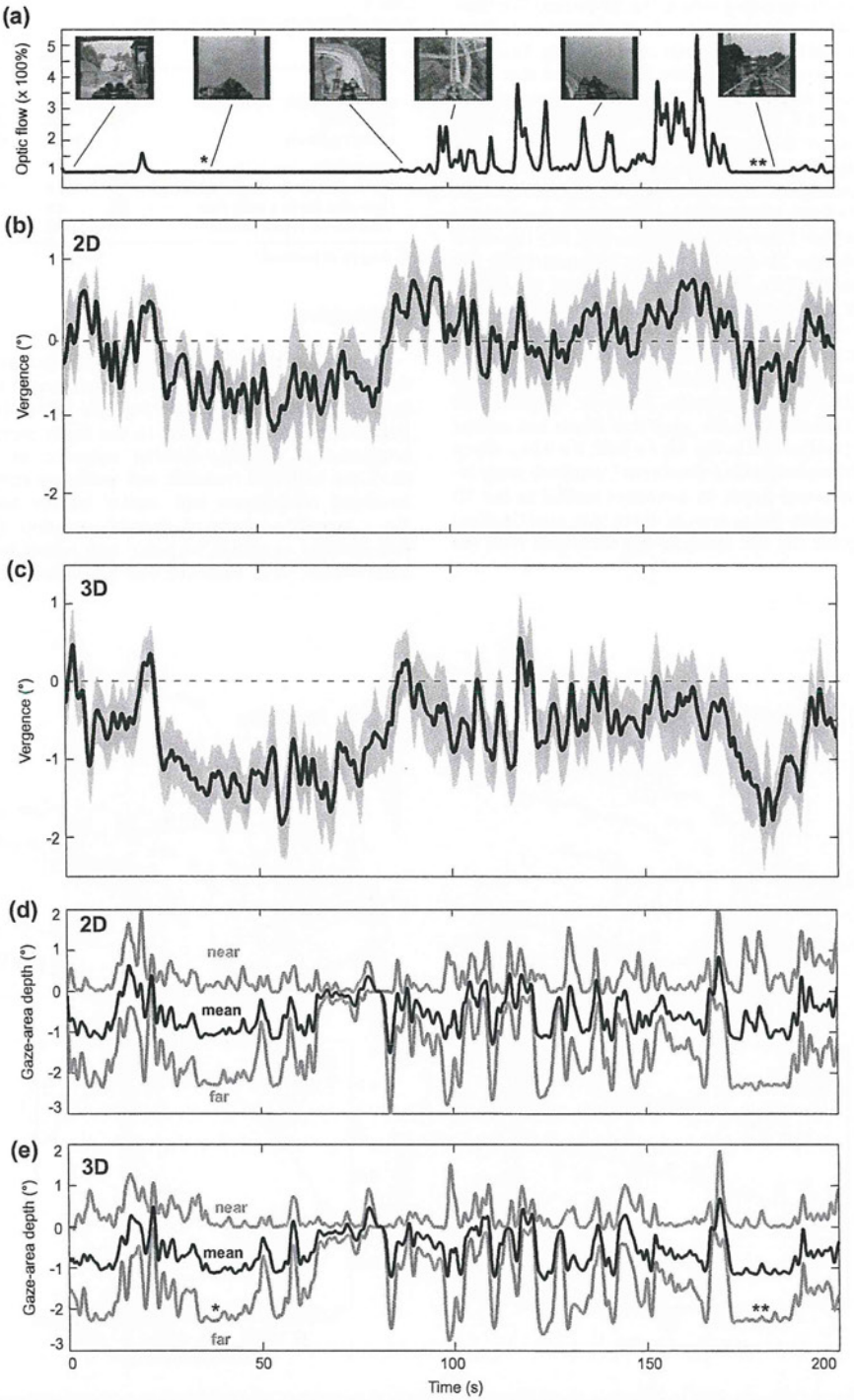

Fig. 2. Persistent and dynamical vergence eye movement induced by a roller coaster video movie. (a) Time course of the optic flow in the video movie and screenshots of the video movie. The roller coaster moved only forward. Radial optic flow above 100% indicates that the optic flow is expanding. (b), (c) Vergence time course during the video movie in 2D (d) and 3D (e) conditions. Black line and shaded area indicate the mean ± SEM ($n = 6$). Dashed lines indicate vergence position at the screen level (0°). Positive and negative values indicate convergence (near) and divergence (far), respectively. Dynamically changing vergence eye movements were reliably induced by the video movie in 2D as well as 3D conditions. (d), (e) Time courses of gaze-area depth in 2D (d) and 3D (e) conditions. The averaged disparity within a 5° × 5° gaze-window was defined as "gaze-area depth" and plotted against time (black line). The upper and lower gray lines indicate the disparity at the nearest and farthest points within the gaze-window, respectively. Asterisks in (a) and (e) indicate the scenes with little optic flow and rich pictorial perspective cues.

disparity within the corresponding area in the 3D picture. We then quantitatively evaluated how vergence was affected by optic flow, the gaze-area depth, and the 2D/3D movie condition (Fig. 3a and b) by conducting three-factor ANOVA (Table 1). We found that optic flow and the gaze-area depth had significant main effects on vergence (optic flow: $F = 9.3$, $P < 0.0001$; gaze-area depth: $F = 24.1$, $P < 0.0001$). The effects of these two factors on vergence were independent, since no significant interactions were observed ($P = 0.26$). No significant interactions were found between optic flow and the movie condition ($P = 0.88$), indicating that optic flow consistently affected vergence in both 2D and 3D conditions (Fig. 3c); the effect would be robust because 2D and 3D movies had essentially the same optic flow contents (Fig. 2b). On the other hand, the effects of gaze-area depth on vergence depended significantly on the movie condition ($F = 22.1$, $P < 0.0001$). In 3D condition, significant positive correlation was found between vergence and the gaze-area depth (solid line in Fig. 3d; $r = 0.84$, partial regression coefficient = 0.033, $P < 0.01$). In 2D condition, however, vergence did not monotonically increase with the gaze area depth but exhibit bimodal responses (broken line in Fig. 3d; $r = 0.92$, $P < 0.01$). When the gaze-area depth was far (behind the screen), vergence angle increased with the gaze-area depth, in a manner similar to the 3D condition. However, when the gaze-area depth was near (in front of the screen) vergence did not increase, but decreased with the gaze-area depth.

Table 1
Result of independent three-factor ANOVA.

Sources	df	*F* value	*P* value	$(Eta\_p)^2$
Main effect				
Gaze-area depth	6	24.1	<0.0001	0.73
Optic flow	11	9.3	<0.0001	0.66
Movie condition	1	144.5	<0.0001	0.73
Interaction				
Gaze-area depth × movie condition	6	22.1	<0.0001	0.71
Gaze-area depth × optic flow	60	1.2	0.26	0.57
Optic flow × movie condition	11	0.5	0.88	0.10

df: Degree of freedom.

4. Discussion

In the present study, we demonstrated that persistent vergence eye movements were induced during prolonged movie stimulation in 2D condition (Figs. 1b and 2c). The basic properties of optic-flow-induced vergence found in our study were consistent with properties of disparity-induced vergence in previous studies [6,19,20]. Both had transient and sustained components and the sustained components had similar latency and rise time (see Fig. 1 legend) to those of disparity vergence [2,21]. The optic-flow-induced sustained vergence was robust from the following observations. First, vergence was maintained through the entire

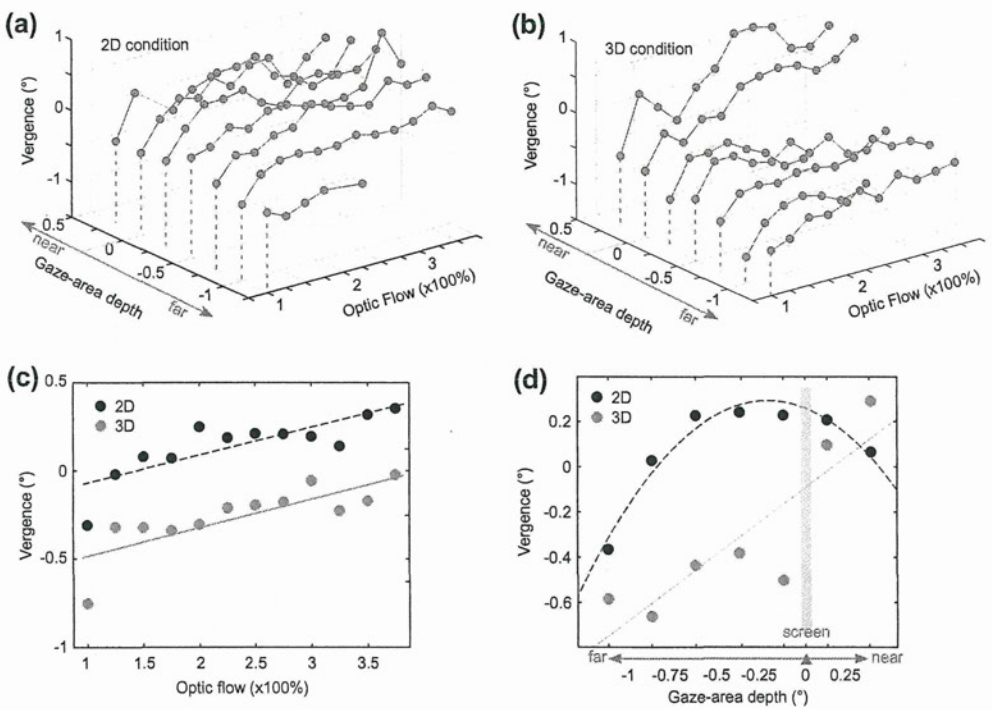

Fig. 3. Effects of optic flow and gaze-area depth on vergence in 2D and 3D movie conditions. (a), (b) Vergence angle during the roller-coaster video movie plotted against optic flow and gaze-area depth for 2D (a) and 3D (b) movie condition. For this plot, the vergence angle data were sorted by a combination of optic flow (12 classes) and the gaze-area depth (7 classes) into 12 × 7 matrix by discarding temporal information. The mean vergence angle in each matrix cell was plotted against optic flow and the gaze-area depth. (c) Vergence angle as a function of optic flow in 2D (black) and 3D (gray) conditions. For this plot, vergence data at 12 optic flow classes were averaged irrespective of gaze-area depth. The dashed (2D) and solid (3D) regression lines were significantly positive (2D, $y = 0.15x - 0.23$, $r = 0.95$, partial regression coefficient = 0.001; 3D, $y = 0.16x - 0.65$, $r = 0.80$, partial regression coefficient = 0.001, where y is vergence and x is optic flow). (d) Vergence angle as a function of gaze-area depth (black, 2D; gray, 3D). The dashed curve and sold line indicate the fitted quadratic curve (2D) and regression line (3D), respectively (2D: $y = -0.73x^2 - 0.31x + 0.26$, $r = 0.93$; 3D: $y = 0.58x - 0.09$, $r = 0.71$).

period of visual motion inputs (Fig. 1b). Second, the vergence responses were highly reproducible across subjects and 2D/3D conditions with little variability (Figs. 1b and c and 2c and d). Third, convergence was automatically induced despite the requirement for fixation on the screen spot (Fig. 1b and c). Fourth, rebound divergence occurred specifically when the subjects reported strong motion after effects with the fixation spot on the screen [22]. It should be noted that no subject reported diplopia due to the gap between the gaze point and the screen, presumably because the gap was within the Panum's fusional area [23]. We speculated that the robustness of optic-flow-induced vergence in our study may be attributable to the faster moving-forward sensation generated by our random-dot movie that simulated roller-coaster motion (70 km/h) unlike prior studies that simulated slow self motion (less than 0.72 km/h) [24].

Vergence is known to originate not only from binocular disparity but also from non-stereoscopic proximal depth cues giving the impression of being nearer or further [2,25]. These cues are typically related to ambiguous optical illusions, and include both static cues [26–28] and motion cues [29,30]. Vergence induced by these cues might be affected by changes in depth perception [26–30], although binocular disparity might be a stronger factor [31]. A sensation of depth can be induced by light and shadow, and laws of perspective on static 2D pictures, which would not necessary associate with vergence eye movement. Our study demonstrates new evidence that the 2D video movie would have provided subjects with unambiguous depth sensation, because continuous vergence was reliably induced and all the subjects reported immersive depth sensations particularly in scenes with strong perspectives and/or fast optic flows. It appeared as if there was a virtual 3D space around the screen despite the 2D presentation. Thus, our findings were basically consistent with the view that non-stereoscopic depth cues induced vergence, and further indicated that vergence would be a persistent sign of the inner representation of depth even in a movie world.

Our study provides the first evidence for simultaneous contributions of binocular disparity, optic flow, and pictorial cues on vergence by comparison of these factors within a single experiment. In both 2D and 3D conditions (Fig. 3a and b), two proximal depth cues, optic flow and the gaze-area depth did not conflict with each other. The discovery of persistent vergence during a 2D movie emphasized the importance of the combination of proximal depth cues, particularly optic flow and the pictorial perspective cue, for providing depth sensations in 3D movies. The asymmetric effects of near and far gaze-area depth on vergence (Fig. 3d) indicate that divergence by the sensation of farness behind the screen may be easily and strongly induced by a 2D movie, whereas convergence by the sensation of nearness in front of the screen might be rather weak. Therefore, making vivid sensation of nearness in virtual reality should be critically dependent on the crossed binocular disparity and the expanding optic flow. In contrast, uncross-disparity for farness might be sufficiently replaced by pictorial perspective cues. In other words, an excessive uncross-disparity added to perspective cues and contracting optic flow could accentuate sensation of farness and cause over-immersive sensation, which might develop several biological effects like motion sickness [3]. These findings impose significant constraints on creation of effective and safe virtual reality environments.

Acknowledgments

We are grateful to M. Takagi and the late K. Ukai for comments on the manuscript. We also thank K. Akazawa and Y. Maeda for statistical advices. This work was supported by grants from JKA through its Promotion funds from KEIRIN RACE and was supported by the Mechanical Social Systems Foundation and the Ministry of Economy, Trade and Industry, Tsukada medical foundation, Foundation for NS sensory research, and Nakayama foundation for human science to A.I., Strategic Research Program for Brain Science and Grant-in-Aid for Scientific Research (C) from The Ministry of Education, Culture, Sports, Science, and Technology, 2008 Specified Research grant from Takeda Science Foundation, Toray Science and Technology Grant of Toray Science Foundation to I.H., and Grants for Promotion of Niigata University Research Project to A.I. and I.H.

Appendix A. Supplementary material

Supplementary data associated with this article can be found, in the online version, at doi:10.1016/j.displa.2011.11.001.

References

[1] D.E. Angelaki, B.J. Hess, Self-motion-induced eye movements: effects on visual acuity and navigation, Nature Reviews Neuroscience 6 (2005) 966–976.
[2] I.P. Howard, B.J. Rogers, Seeing in Depth, Oxford University Press, 2008.
[3] R.H.Y. So, W.T. Lo, A.T.K. Ho, Scene movement: an important cause of cybersickness, in: H.M. Khalid, M. Helander (Eds.), Virtual Reality, Academic Press, 2000.
[4] C. Schor, K.M. Robertson, M. Wesson, Disparity vergence dynamics and fixation disparity, American journal of optometry and physiological optics 63 (1986) 611–618.
[5] J. Semmlow, P. Wetzel, Dynamic contributions of the components of binocular vergence, Journal of the Optical Society of America 69 (1979) 639–645.
[6] D.S. Zee, L. Levi, Neurological aspects of vergence eye movements, Revue Neurologique 145 (1989) 613–620.
[7] J.P. Wann, S. Rushton, M. Mon-Williams, Natural problems for stereoscopic depth perception in virtual environments, Vision Research 35 (1995) 2731–2736.
[8] Y. Hayakawa, M. Takagi, A. Iijima, T. Bando, R. Takada, A. Miki, T. Usui, S. Hasegawa, H. Abe, Effect of the background on the disparity-induced ramp vergence response in humans, ophthalmologica, Journal International d'ophtalmologie. International Journal of Ophthalmology 220 (2006) 94–100.
[9] N. Li, D.E. Angelaki, Updating visual space during motion in depth, Neuron 48 (2005) 149–158.
[10] T. Fukushima, M. Torii, K. Ukai, J.S. Wolffsohn, B. Gilmartin, The relationship between CA/C ratio and individual differences in dynamic accommodative responses while viewing stereoscopic images, Journal of Vision 9 (2009). 21–13.
[11] J.J. Gibson, The Perception of the Visual World, Houghton Mifflin, Oxford, 1950.
[12] M. Lappe, Neuronal Processing of Optic Flow, Academic Press, CA, USA, 1999.
[13] C. Busettini, G.S. Masson, F.A. Miles, Radial optic flow induces vergence eye movements with ultra-short latencies, Nature 390 (1997) 512–515.
[14] K. Kawano, Ocular tracking: behavior and neurophysiology, Current Opinion in Neurobiology 9 (1999) 467–473.
[15] I. Hasegawa, T. Fukushima, T. Ihara, Y. Miyashita, Callosal window between prefrontal cortices: cognitive interaction to retrieve long-term memory, Science 281 (1998) 814–818.
[16] A. Iijima, H. Minamitani, N. Ishikawa, Image analysis of quick phase eye movements in nystagmus with high-speed video system, Medical and Biological Engineering and Computing 39 (2001) 2–7.
[17] F.A. Proudlock, I. Gottlob, Physiology and pathology of eye-head coordination, Progress in Retinal and Eye Research 26 (2007) 486–515.
[18] J.Y.A. Wang, E.H. Adelsen, Representing moving images with layers, IEEE Transactions on Image Processing 3 (1994) 625–638.
[19] J.L. Semmlow, G.K. Hung, K.J. Ciuffreda, Quantitative assessment of disparity vergence components, Investigative Ophthalmology and Visual Science 27 (1986) 558–564.
[20] T. Bando, N. Hara, M. Takagi, H. Hasebe, R. Takada, H. Toda, Vergence eye movement and lens accommodation: cortical processing and neuronal pathway, in: O. Franzen, H. Richter, L. Stark (Eds.), Accommodation and Vergence Mechanisms in the Visual System, Birkhaeuser Basel, 2000, pp. 44–50.
[21] V.V. Krishnan, S. Phillips, L. Stark, Frequency analysis of accommodation, accommodative vergence and disparity vergence, Vision Research 13 (1973) 1545–1554.
[22] A. Rezec, B. Krekelberg, K.R. Dobkins, Attention enhances adaptability: evidence from motion adaptation experiments, Vision research 44 (2004) 3035–3044.
[23] K.N. Ogle, On the limits of stereoscopic vision, Journal of Experimental Psychology 44 (1952) 253–259.
[24] M. Zhu, R.W. Hertle, D. Yang, Relationships between versional and vergent quick phases of the involuntary version-vergence nystagmus, Journal of vision 8 (2008). 11 11–11.
[25] W.H. Warren Jr., D.J. Hannon, Direction of self-motion is perceived from optical flow, Nature 336 (1988) 162–163.
[26] J.T. Enright, Art and the oculomotor system: perspective illustrations evoke vergence changes, Perception 16 (1987) 731–746.

[27] J.T. Enright, Perspective vergence: oculomotor responses to line drawings, Vision Research 27 (1987) 1513–1526.
[28] B.M. Sheliga, F.A. Miles, Perception can influence the vergence responses associated with open-loop gaze shifts in 3D, Journal of Vision 3 (2003) 654–676.
[29] I.P. Howard, Vergence modulation as a cue to movement in depth, Spatial Vision 21 (2008) 581–592.
[30] D.L. Ringach, M.J. Hawken, R. Shapley, Binocular eye movements caused by the perception of three-dimensional structure from motion, Vision Research 36 (1996) 1479–1492.
[31] D.A. Wismeijer, R. van Ee, C.J. Erkelens, Depth cues, rather than perceived depth, govern vergence, Experimental Brain Research. Experimentelle Hirnforschung 184 (2008) 61–70.

International Journal of
Radiation Oncology
biology • physics

www.redjournal.org

Clinical Investigation: Central Nervous System Tumor

Integration of Corticospinal Tractography Reduces Motor Complications After Radiosurgery

Tomoyuki Koga, M.D.,* Masahiro Shin, M.D.,* Keisuke Maruyama, M.D.,* Kyousuke Kamada, M.D.,* Takahiro Ota, M.D.,* Daisuke Itoh, M.D.,† Naoto Kunii, M.D.,* Kenji Ino, R.T.,† Shigeki Aoki, M.D.,† Yoshitaka Masutani, Ph.D.,† Hiroshi Igaki, M.D.,† Tsuyoshi Onoe, M.D.,† and Nobuhito Saito, M.D.*

*Departments of *Neurosurgery and †Radiology, The University of Tokyo Hospital, Tokyo, Japan*

Received Mar 25, 2011. Accepted for publication May 17, 2011

Summary

When diffusion-tensor tractography is integrated into stereotactic radiosurgery for brain arteriovenous malformations adverse events may be reduced although the effect on AVM obliteration rates is unknown. This study compared outcomes of patients treated with and without tractography. The integration of tractography of the corticospinal tract significantly reduced motor complication without compromising obliteration rate.

Purpose: To evaluate whether the use of diffusion-tensor tractography (DTT) of the corticospinal tract could reduce motor complications after stereotactic radiosurgery (SRS).
Methods and Materials: Patients with arteriovenous malformation (AVM) in the deep frontal lobe, deep parietal lobe, basal ganglia, and thalamus who had undergone radiosurgery since 2000 and were followed up for more than 3 years were studied. DTT of the corticospinal tract had been integrated into treatment planning of SRS since 2004, and the maximum dose received by the corticospinal tract was attempted to be less than 20 Gy. Treatment outcomes before (28 patients, Group A) and after (24 patients, Group B) the introduction of this technique were compared.
Results: There were no statistical differences between the two groups (Group A vs. Group B) in patients' age (34 years vs. 33 years, $p = 0.76$), percentage of patients with hemorrhagic events before treatment (50% vs. 29%, $p = 0.12$), or percentage of AVM involving the basal ganglia and thalamus (36% vs. 46%, $p = 0.46$). Obliteration rates were 69% and 76% at 4 years in Groups A and B, respectively ($p = 0.68$), which were not significantly different. Motor complications were observed in 5 patients in Group A (17.9%) but only in 1 patient in Group B (4.2%), which was significantly less frequent ($p = 0.021$).
Conclusion: Integrating DTT of the corticospinal tract into treatment planning contributed to reduction of motor complications without compromising the obliteration rate for AVM adjacent to the corticospinal tract.

Keywords: Arteriovenous malformation, Corticospinal tract, Diffusion-tensor tractography, Morbidity, Stereotactic radiosurgery

Introduction

Stereotactic radiosurgery (SRS) is widely accepted as a treatment modality for brain disorders including brain neoplasms, vascular lesions, and functional disorders (1–5). Although SRS is known as one of the least invasive treatment modalities for cerebral arteriovenous malformations (AVM), the associated risk of radiation-induced neuropathy occurs in 5–20% of patients

Reprint requests to: Tomoyuki Koga, M.D., Department of Neurosurgery, The University of Tokyo Hospital, 7-3-1 Hongo, Bunkyo-ku, Tokyo 113-8655, Japan. Tel: (+81) 3-5800-8853; Fax: (+81) 3-5800-8655; E-mail: kouga-tky@umin.ac.jp

Conflict of interest: none.

Int J Radiation Oncol Biol Phys, Vol. 83, No. 1, pp. 129–133, 2012
0360-3016/$ - see front matter
doi:10.1016/j.ijrobp.2011.05.036

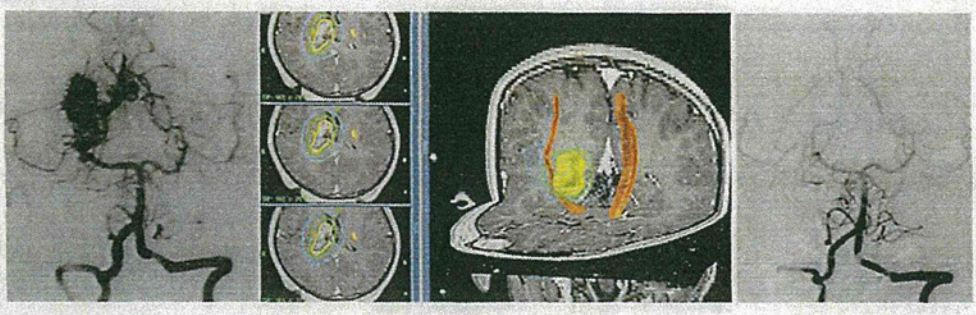

Fig. 1. Cerebral angiogram of a patient with right thalamic arteriovenous malformation (left). Treatment planning of radiosurgery with integration of diffusion-tensor tractography of the corticospinal tract (orange, middle). Cerebral angiogram taken at 36 months after treatment showed complete obliteration without any adverse event (right).

(3, 6–9), which is not negligible for patients with AVM in deep-seated eloquent areas. To minimize such risk, we have integrated tractography of the brain white matter based on diffusion-tensor magnetic resonance imaging (MRI) into treatment planning of SRS using the Gamma Knife (10–12). Diffusion tensor tractography (DTT), one of the major recent advancements in MRI, enables clear visualization of various fibers inside the white matter of the brain that are not visible with conventional imaging methods (13). Until now, we have used this technology in SRS for more than 100 patients with AVM in the eloquent areas. However, it is still not clear whether modification of dose planning based on DTT has contributed to reduction of associated morbidity or how much the obliteration rate was affected by it. To clarify these issues, we analyzed the effect of integrating DTT of the corticospinal tract into treatment planning on neurologic complications and obliteration rates after SRS.

Methods and Materials

Patients

The data from patients with AVM in the deep frontal lobe, deep parietal lobe, basal ganglia, and thalamus were retrospectively analyzed because most of the lesions in these locations were considered to be close to the corticospinal tract and were classified as the eloquent area. After SRS, it usually takes 3 to 5 years to achieve radiographic obliteration of the treated AVM nidus (14). Thus, to evaluate obliteration rates, patients who were followed up for at least 3 years were included in this study.

We analyzed the outcomes in 52 patients with AVM in the deep frontal lobe, deep parietal lobe, basal ganglia, and thalamus after January 2000, in whom the same dose planning soft and imaging methods were used at SRS except for the use of DTT. Between January 2000 and January 2004, 28 patients were treated without the use of DTT (Group A). For these patients, after head fixation using a Leksell stereotactic frame, MRI and cerebral angiography were performed. Conformal treatment planning was made by the neurosurgeon and the radiation oncologist with the sophisticated software GammaPlan (15). All the patients in this group were treated by using a margin dose of 20 Gy or more. Since February 2004, we have begun to integrate DTT of the corticospinal tract, and 24 patients with those AVM were treated. Diffusion-tensor MRI was obtained on the day before treatment. Tractography was created from diffusion-tensor imaging by using freely shared programs, based on anatomic landmarks as shown in previous studies (10–13).

Standard protocol approval, registration, and patient consent

The study was approved by the institutional review board at the University of Tokyo Hospital. Informed consent was obtained from all patients participating in the study.

Procedures

On the day of treatment, patients were affixed to the stereotactic coordinate frame and underwent MRI and cerebral angiography. Then the MRI was registered by using the method as previously reported (10–12, 16). After the introduction of Gamma Knife 4C in October 2006, the registration process was automatized (17). Tractography-integrated images were imported to treatment planning software on the day of the treatment. Conformal treatment planning was made by experienced neurosurgeons and radiation oncologists by using treatment planning software GammaPlan. Radiotherapy of 15 to 20 Gy (median, 20 Gy) was given to the margin of the lesions by using 40–50% isodose lines, according to

Table 1 Comparison of characteristics of the patients in Groups A and B

Characteristic	Group A	Group B	*p* value
Number of patients	28	24	–
Patient age (y) (mean, range)	34, 8–64	33, 11–64	0.76
Hemorrhage before treatment	14 (50%)	7 (29%)	0.12
Basal ganglia or thalamus	10 (36%)	11 (46%)	0.46
Treated volume (cm^3) (mean, range)	4.8, 0.2–13.7	7.7, 1.1–22.4	0.026

Table 2 Factors associated with angiographically confirmed obliteration of the arteriovenous malformation nidus after stereotactic radiosurgery

Factor	*p* value
Group A	0.70
Younger patient age	0.13
Hemorrhage before treatment	0.49
Location other than the basal ganglia and thalamus	0.12
Smaller treated volume	0.42

the volume of the nidus. The precise location of the corticospinal tract was confirmed on treatment planning images, and the maximum dose received by the corticospinal tract was restricted to be less than 20 Gy on the basis of previous analyses (Fig. 1) (10–12).

Follow-up and statistical analysis

Serial formal neurologic and radiologic examinations were performed every 6 months after the procedure. The outcomes including motor complications, other adverse events, and complete obliteration confirmed by cerebral angiography were compared between Groups A and B. Statistical analyses were performed using JMP 8 (SAS Institute Inc., Cary, NC). Comparisons of patients' age, nidus volume, and follow-up period were performed by two-sample *t* test. The rate of motor complications and other adverse events and the actuarial obliteration rate were calculated using the Kaplan-Meier method. The rates of adverse events and obliteration rates of patients in both groups were compared using the Cox proportional hazard model.

Results

Comparison of the two groups

The patient characteristics and treatments in both groups are summarized in Table 1. There were no statistical difference between the two groups (Group A vs. Group B) in patients' age at treatment (34 years vs. 33 years, $p = 0.76$), percentage of patients with hemorrhagic events before treatment (50% vs. 29%), or percentage of AVM involving the basal ganglia and thalamus (36% vs. 46%, $p = 0.46$). The treated volume was significantly smaller ($p = 0.026$) in Group A (mean, 4.8 cm^3; range, 0.2–13.7 cm^3) than in Group B (mean, 7.7 cm^3; range, 1.1–22.4 cm^3), and the applied marginal dose was lower in Group B (mean, 19.6 Gy; range, 15–20 Gy) than in Group A (mean, 20.2 Gy; range, 20–25 Gy). The median follow-up period was 62 months (range, 36–113 months) in Group A and 48 months (range, 36–80 months) in Group B ($p = 0.004$).

Nidus obliteration

Angiographically confirmed nidus obliteration rates at 4 years after SRS was 69% in Group A and 76% in Group B. Integration of DTT was not significantly associated with obliteration rate ($p = 0.68$) (Table 2). Latency interval hemorrhage after treatment occurred in 1 patient, in whom no worsening of neurologic symptom was observed.

Complications

During the follow-up period, neurologic events occurred in 9 patients, 6 in Group A and 3 in Group B (Table 3). In Group A, transient hemiparesis was observed in 3 patients, permanent hemiparesis in 1, permanent dysesthesia in 1, and both permanent hemiparesis and dysesthesia in 1 patient. Modified Rankin Scale scores at last follow-up in these 6 patients were 0 in 3 patients, 1 in 1 patient, and 2 in 2 patients. In Group B, transient hemiparesis, permanent dysesthesia, and transient motor aphasia were observed in 1 patient each. Modified Rankin Scale scores at the last follow-up in these 4 patients were 0 in 3 patients and 1 in 1 patient. Deterioration of modified Rankin Scale scores at the last follow-up was observed in 3 patients among the 6 patients in Group A and 1 patient among 3 patients in Group B.

When we analyzed factors associated with the risk of neurologic events after SRS, integration of DTT of the corticospinal tract did not significantly ameliorate the overall risks of any kind of morbidity ($p = 0.18$), and involvement of the basal ganglia or thalamus was solely associated with higher risks ($p = 0.007$) (Table 4).

However, focusing on motor complications, Group A or the use of DTT of the corticospinal tract was significantly associated with a lower rate of motor complications ($p = 0.021$) (Table 5). Namely, it indicated that SRS using DTT of the corticospinal tract at dose planning could significantly reduce those risks (5 patients in Group A vs. 1 in Group B).

Table 3 Characteristics of patients who experienced neurologic deterioration after stereotactic radiosurgery

Age/sex	Group	Nidus location	Nidus volume (cm^3)	Margin dose (Gy)	Timing of obliteration (mo)	Follow-up period (mo)	Kind of morbidity	Timing of morbidity (mo)	MRS at last follow-up
26/F	A	Thalamus	9.2	20	35	60	Hemiparesis/dysesthesia	4	2
64/M	A	Frontal lobe	2.0	20	ND	46	Transient hemiparesis	11	0
24/M	A	Thalamus	2.5	20	36	39	Permanent dysesthesia	1	1
11/M	A	Thalamus	12.3	20	39	87	Permanent hemiparesis	11	2
20/F	A	Basal ganglia	0.4	20	38	38	Transient hemiparesis	16	0
28/M	A	Frontal lobe	8.5	20	36	36	Transient hemiparesis	16	0
48/M	B	Basal ganglia	12.9	20	44	63	Transient aphasia	2	0
14/F	B	Thalamus	5.3	20	46	46	Permanent dysesthesia	10	1
25/F	B	Basal ganglia	13.0	18	24	36	Transient hemiparesis	11	0

Abbreviations: MRS = modified Rankin Score; ND = data not available.

Table 4 Factors associated with any kind of morbidity after stereotactic radiosurgery

Factor	*p* value
Group A	0.18
Older patient age	0.33
Larger treated volume	0.17
Involvement of the basal ganglia or thalamus	0.007

Table 5 Factors associated with motor complications after stereotactic radiosurgery

Factor	*p* value
Group A	0.021
Older patient age	0.71
Larger treated volume	0.091
Involvement of the basal ganglia or thalamus	0.065

In the patient who had transient hemiparesis in Group B, the volume of AVM nidus that was located in the basal ganglia was relatively large: 13.0 cm^3. The lesion was treated with a margin dose of 18 Gy, and the maximum dose delivered to the corticospinal tract was 17 Gy (Fig. 2).

Discussion

Since the introduction of DTT-integrated SRS, we have partially modified treatment dose planning at SRS for AVM (10–12, 16) to restrict the irradiation dose to the adjacent motor fibers, and our early data suggested that SRS with integration of DTT was likely to be useful to prevent radiation-induced adverse events in AVM patients (10, 11, 18). With the accumulation of cases and the follow-up in this study, we evaluated the substantial effects of this technique because two principal concerns still remained unknown: whether integration of DTT could actually eliminate the risk of radiation-induced motor complications in any AVM patients, and how much such dose modifications would affect the other therapeutic effects such as nidus obliteration rates. Our results showed that SRS with DTT of the corticospinal tract could significantly reduce associated radiation-induced motor complications without affecting the nidus obliteration rates, proving that it contributes to preventing one of the most undesirable complications of SRS for AVM.

However, 1 patient had a large nidus involving the basal ganglia and experienced transient hemiparesis after DTT-integrated SRS, which raised another issue. In this patient, the maximum dose received by the corticospinal tract was less than 20 Gy, which had been considered as a tolerable dose to the motor fibers in our preliminary results (10, 11). Larger nidus volume might have exposed the larger portion of the corticospinal tract to a relatively high dose even though the maximum dose did not surpass the tolerable dose, and this might have caused the hemiparesis. Also, the motor fibers passing through the internal capsule, close to the basal ganglia, are assembled in relatively small territories and are more likely to be affected than are fibers close to the cortical areas (10). Therefore, we speculate that the maximum dose to the corticospinal tract is not the only factor in the development of motor complications after SRS, but the extent of irradiated volume of the motor fibers and the irradiated part can be also associated with them as previously analyzed (10).

DTT has been widely used, and its usefulness has been established especially as a diagnostic tool (19). However, the major concern with regard to tractography is its reliability. If the tracts are not shown on the image, that does not always mean that the fibers do not exist (19, 20). By contrast, it has been shown by intraoperative fiber stimulation analysis that the tracts seen on DTT reflect the functioning white matter fibers to some extent (21). Furthermore, those imaging methods are suitable for SRS because SRS has no risk of brain shift caused by craniotomy or

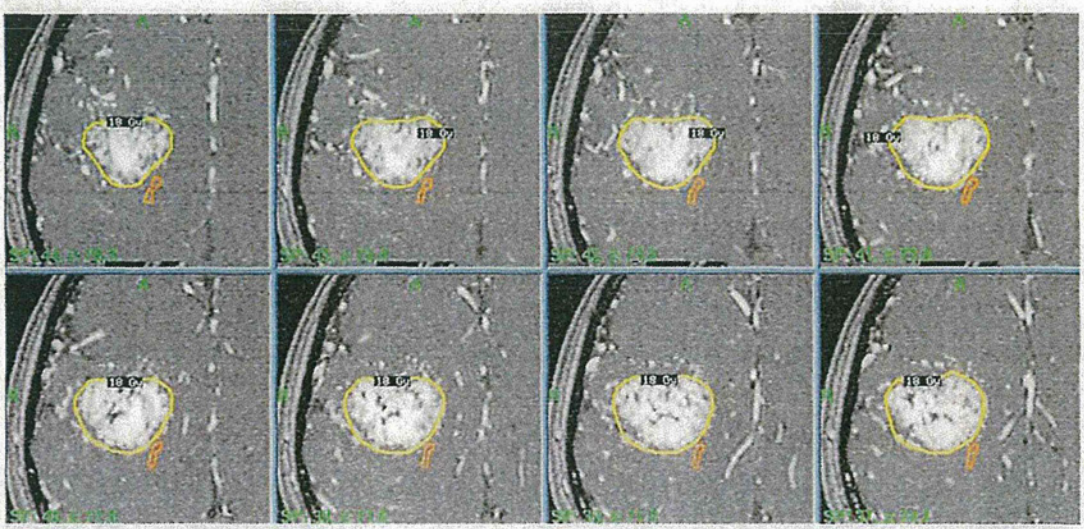

Fig. 2. Treatment planning for a patient with right frontal arteriovenous malformation who experienced transient left hemiparesis after radiosurgery. Long portion of the corticospinal tract (orange) was located adjacent to the large nidus.

tumor removal, which is inevitable in intraoperative applications (22).

The obliteration rates in the cohort in this study, which were 69–76 % at 4 years, were relatively low compared with those previously published (14). Inasmuch as it has been reported that obliteration rates of deeply located AVM have been low, 57–74% within 3 to 4 years (8, 23, 24), and that the lesions in 36–46% of the patients in this study were deeply located AVM, the lower obliteration rates might be explained by patient selection.

Further accumulation of cases with longer follow-up data is awaited to evaluate the effect of integrating tractography into Gamma Knife SRS, but our study disclosed that integrating DTT of the corticospinal tract into treatment planning at SRS contributed to reduction of motor complications and achieved safer treatment without compromising the obliteration rate for AVM adjacent to motor fibers.

References

1. Koga T, Shin M, Saito N. Role of gamma knife radiosurgery in neurosurgery: Past and future perspectives. *Neurol Med Chir (Tokyo)* 2010;50:737–748.
2. Leksell L. Cerebral radiosurgery. I. Gammathalamotomy in two cases of intractable pain. *Acta Chir Scand* 1968;134:585–595.
3. Maruyama K, Kawahara N, Shin M, *et al.* The risk of hemorrhage after radiosurgery for cerebral arteriovenous malformations. *N Engl J Med* 2005;352:146–153.
4. Maruyama K, Kondziolka D, Niranjan A, *et al.* Stereotactic radiosurgery for brainstem arteriovenous malformations: Factors affecting outcome. *J Neurosurg* 2004;100:407–413.
5. Maruyama K, Shin M, Kurita H, *et al.* Proposed treatment strategy for cavernous sinus meningiomas: A prospective study. *Neurosurgery* 2004;55:1068–1075.
6. Andrade-Souza YM, Zadeh G, Scora D, *et al.* Radiosurgery for basal ganglia, internal capsule, and thalamus arteriovenous malformation: Clinical outcome. *Neurosurgery* 2005;56:56–64.
7. Flickinger JC, Kondziolka D, Lunsford LD, *et al.* A multi-institutional analysis of complication outcomes after arteriovenous malformation radiosurgery. *Int J Radiat Oncol Biol Phys* 1999;44:67–74.
8. Pollock BE, Gorman DA, Brown PD. Radiosurgery for arteriovenous malformations of the basal ganglia, thalamus, and brainstem. *J Neurosurg* 2004;100:210–214.
9. Sasaki T, Kurita H, Saito I, *et al.* Arteriovenous malformations in the basal ganglia and thalamus: Management and results in 101 cases. *J Neurosurg* 1998;88:285–292.
10. Maruyama K, Kamada K, Ota T, *et al.* Tolerance of pyramidal tract to gamma knife radiosurgery based on diffusion-tensor tractography. *Int J Radiat Oncol Biol Phys* 2008;70:1330–1335.
11. Maruyama K, Kamada K, Shin M, *et al.* Integration of three-dimensional corticospinal tractography into treatment planning for gamma knife surgery. *J Neurosurg* 2005;102:673–677.
12. Maruyama K, Kamada K, Shin M, *et al.* Optic radiation tractography integrated into simulated treatment planning for Gamma Knife surgery. *J Neurosurg* 2007;107:721–726.
13. Masutani Y, Aoki S, Abe O, *et al.* MR diffusion tensor imaging: Recent advance and new techniques for diffusion tensor visualization. *Eur J Radiol* 2003;46:53–66.
14. Shin M, Maruyama K, Kurita H, *et al.* Analysis of nidus obliteration rates after gamma knife surgery for arteriovenous malformations based on long-term follow-up data: The University of Tokyo experience. *J Neurosurg* 2004;101:18–24.
15. Koga T, Shin M, Maruyama K, *et al.* Long-term outcomes of stereotactic radiosurgery for arteriovenous malformations in the thalamus. *Neurosurgery* 2010;67:398–403.
16. Maruyama K, Koga T, Kamada K, *et al.* Arcuate fasciculus tractography integrated into Gamma Knife surgery. *J Neurosurg* 2009;111:520–526.
17. Koga T, Maruyama K, Igaki H, *et al.* The value of image coregistration during stereotactic radiosurgery. *Acta Neurochir (Wien)* 2009;151:465–471. discussion 471.
18. Koga T, Maruyama K, Kamada K, *et al.* Outcomes of diffusion tensor tractography-integrated stereotactic radiosurgery. *Int J Radiat Oncol Biol Phys*, In press.
19. Yamada K, Sakai K, Akazawa K, *et al.* MR tractography: A review of its clinical applications. *Magn Reson Med Sci* 2009;8:165–174.
20. Holodny AI, Watts R, Korneinko VN, *et al.* Diffusion tensor tractography of the motor white matter tracts in man: Current controversies and future directions. *Ann N Y Acad Sci* 2005;1064:88–97.
21. Kamada K, Todo T, Ota T, *et al.* The motor-evoked potential threshold evaluated by tractography and electrical stimulation. *J Neurosurg* 2009;111:785–795.
22. Kamada K, Todo T, Masutani Y, *et al.* Combined use of tractography-integrated functional neuronavigation and direct fiber stimulation. *J Neurosurg* 2005;102:664–672.
23. Kiran NA, Kale SS, Kasliwal MK, *et al.* Gamma knife radiosurgery for arteriovenous malformations of basal ganglia, thalamus and brainstem: A retrospective study comparing the results with that for AVMs at other intracranial locations. *Acta Neurochir (Wien)* 2009;151:1575–1582.
24. Andrade-Souza YM, Zadeh G, Scora D, *et al.* Radiosurgery for basal ganglia, internal capsule, and thalamus arteriovenous malformation: Clinical outcome. *Neurosurgery* 2005;56:56–63. discussion 63–54.

Int. J. Radiation Oncology Biol. Phys., Vol. 82, No. 2, pp. 799–802, 2012

0360-3016/$ - see front matter

ELSEVIER

doi:10.1016/j.ijrobp.2010.11.046

CLINICAL INVESTIGATION **Central Nervous System Tumor**

OUTCOMES OF DIFFUSION TENSOR TRACTOGRAPHY–INTEGRATED STEREOTACTIC RADIOSURGERY

TOMOYUKI KOGA, M.D.,* KEISUKE MARUYAMA, M.D., PH.D.,* KYOUSUKE KAMADA, M.D., PH.D.,* TAKAHIRO OTA, M.D., PH.D.,* MASAHIRO SHIN, M.D., PH.D.,* DAISUKE ITOH, M.D., PH.D.,† NAOTO KUNII, M.D.,* KENJI INO, R.T.,† ATSURO TERAHARA, M.D., PH.D.,† SHIGEKI AOKI, M.D., PH.D.,† YOSHITAKA MASUTANI, PH.D.,† AND NOBUHITO SAITO, M.D., PH.D.*

Departments of *Neurosurgery and †Radiology, University of Tokyo Hospital, Tokyo, Japan

Purpose: To analyze the effect of use of tractography of the critical brain white matter fibers created from diffusion tensor magnetic resonance imaging on reduction of morbidity associated with radiosurgery.
Methods and Materials: Tractography of the pyramidal tract has been integrated since February 2004 if lesions are adjacent to it, the optic radiation since May 2006, and the arcuate fasciculus since October 2007. By visually confirming the precise location of these fibers, the dose to these fiber tracts was optimized. One hundred forty-four consecutive patients with cerebral arteriovenous malformations who underwent radiosurgery with this technique between February 2004 and December 2009 were analyzed.
Results: Tractography was prospectively integrated in 71 of 155 treatments for 144 patients. The pyramidal tract was visualized in 45, the optic radiation in 22, and the arcuate fasciculus in 13 (two tracts in 9). During the follow-up period of 3 to 72 months (median, 23 months) after the procedure, 1 patient showed permanent worsening of preexisting dysesthesia, and another patient exhibited mild transient hemiparesis 12 months later but fully recovered after oral administration of corticosteroid agents. Two patients had transient speech disturbance before starting integration of the arcuate fasciculus tractography, but no patient thereafter.
Conclusion: *Integrating tractography helped prevent morbidity of radiosurgery in patients with brain arteriovenous malformations.* © 2012 Elsevier Inc.

Arteriovenous malformation, Diffusion tensor tractography, Gamma knife, Morbidity, Stereotactic radiosurgery.

INTRODUCTION

Stereotactic radiosurgery is one of the principal treatment modalities for various kinds of vascular, neoplastic, or functional disorders of the brain (1–4). Although its efficacy is well known, radiation-induced neuropathy occurs in 5–20% of patients (2, 5–8). To minimize such unignorable risk, we have integrated tractography of the brain white matter based on diffusion tensor magnetic resonance imaging before the procedure into treatment planning of radiosurgery using Gamma Knife (9–11). Diffusion tensor tractography, one of the major recent advancements in magnetic resonance imaging, enables clear visualization of various fibers inside the white matter of the brain, which is not visible with use of conventional imaging modalities (12). Clinical applications of diffusion tensor tractography are mainly reported as diagnostic tools, and reports on its therapeutic application are quite limited (10, 13). In this study, we analyzed the effect of integrating diffusion tensor tractography into treatment planning of stereotactic radiosurgery on the reduction of morbidity in a prospective case series with arteriovenous malformations of the brain.

METHODS AND MATERIALS

Our selection criterion for stereotactic radiosurgery was, in principle, small malformations (<3 cm) in critical, or eloquent, areas of the brain (including sensorimotor, language, or visual cortex; the hypothalamus or thalamus; the internal capsule; the brain stem; the cerebellar peduncles; and the deep cerebellar nuclei) that, if injured, result in disabling neurologic deficits (2, 14). We started integrating diffusion tensor tractography of the pyramidal tract in February 2004 because we considered the pyramidal tract to be the most crucial fiber in preventing morbidity of radiosurgery out of complexity of white matter fibers inside the brain. From May 2006, we added the integration of diffusion tensor tractography of the optic radiation, and diffusion tensor tractography of the arcuate fasciculus tractography from October 2007. One hundred forty-four patients with arteriovenous malformations who have consecutively undergone stereotactic radiosurgery using Gamma Knife with this protocol between February 2004 and December

Reprint requests to: Tomoyuki Koga, M.D., Department of Neurosurgery, University of Tokyo Hospital, 7-3-1 Hongo, Bunkyo-ku, Tokyo 113-8655, Japan. Tel: (+81) 3-5800-8853; Fax: (+81) 3-5800-8655; E-mail: kouga-tky@umin.ac.jp

Conflicts of interest: none.
Received Sept 22, 2010, and in revised form Sept 22, 2010. Accepted for publication Nov 4, 2010.

Table 1. Baseline characteristics of 144 patients treated

Age (y)	35 (5–77)
Female sex	65 (45)
Details of arteriovenous malformations	
Diameter (cm)	2.7 (0.7–7.9)
Small size	89 (62)
Eloquent brain location	66 (46)
Deep venous drainage	74 (51)
Spetzler-Martin grade	II (I–VI)
Details of radiosurgery	
Target volume (cm^3)	6.9 (0.3–24)
Maximal dose (Gy)	40 (32–50)
Dose to margins (Gy)	20 (15–25)
Follow-up period (mo)	23 (3–72)

Data are number (percentage) or median (range).

2009 were enrolled in this study. All patients were considered as candidates for integrating tractography, but the integration was not carried out if a target lesion was considered to be located more than 1 cm apart from these fiber tracts and risk of injuring them was considered to be sufficiently low. Malformations were located in eloquent brain areas in 66 patients (46%). Detailed treatment parameters are shown in Table 1.

Diffusion tensor magnetic resonance imaging was obtained on the day before treatment. Tractography was created from diffusion tensor imaging by using freely shared programs, according to anatomic landmarks as shown in previous studies (9–12).

On the day of treatment, patients were affixed to the stereotactic coordinate frame and underwent stereotactic magnetic resonance imaging and stereotactic cerebral angiography. Stereotactic magnetic resonance imaging and tractography were registered by using the method reported previously (9–11, 15). After the introduction of Gamma Knife 4C in October 2006, the registration process was automated (16). Tractography-integrated images were imported to treatment planning images on the day of radiosurgery. Conformal treatment planning was made by experienced neurosurgeons and radiation oncologists with use of the treatment planning software GammaPlan (Elekta Instruments AB, Stockholm, Sweden). Generally 20 Gy was given to the margin of lesions by using 40–50% isodose lines. Any portion of the anterior visual pathway and half of the brainstem were designed to receive no more than 10 Gy.

The precise location of the pyramidal tract (Fig. 1), the optic radiation (Fig. 2), or the arcuate fasciculus was confirmed on treatment planning images, and it was attempted that the maximum dose received by each fiber was less than 20 Gy, 8 Gy, or 8 Gy (20 Gy in the frontal fibers), respectively, on the basis of previous analyses (9–11), though this was not possible in some cases.

Serial formal neurologic and radiologic examination was performed every 6 months after the procedure.

RESULTS

Diffusion tensor–based tractography was prospectively integrated in 71 (46%) of 155 treatment sessions. Integrated fiber tracts were the pyramidal tract in 45, the optic radiation in 22, and the arcuate fasciculus in 13 sessions, including 9 in which two tracts were integrated (the pyramidal tract and the optic radiation in 2, the pyramidal tract and the arcuate fasciculus in 3, the optic radiation and the arcuate fasciculus in 4). The optic radiation could not be depicted in 1 patient, and only arcuate fasciculus was drawn. Of 71 treatments with integration of tractography, the distance between the lesion and critical white matter fibers was less than 5 mm in 43 (60%); thus, tighter treatment planning was mandatory. Consequently, 39 sessions (55%) necessitated any modification in treatment planning by reducing the radiation dose to the visualized tracts. Until December 2007, 38% of treatments (37 of 98 sessions) were performed with integration of tractography, whereas tractography was integrated for 60% (34 of 57) thereafter. This difference in frequency was statistically significant according to χ^2 test ($p = 0.008$).

Two patients died of unknown cause after the procedure. The other 142 patients were followed for 3–72 months (median, 23 months) after radiosurgery. During this period, transient speech disturbance was observed in 2 patients. They were treated before 2007, when we started integrating arcuate fasciculus tractography. One patient with right thalamic arteriovenous malformation showed gradual worsening of pre-existing dysesthesia of left upper and lower extremities after treatment, and this symptom lasted until the last

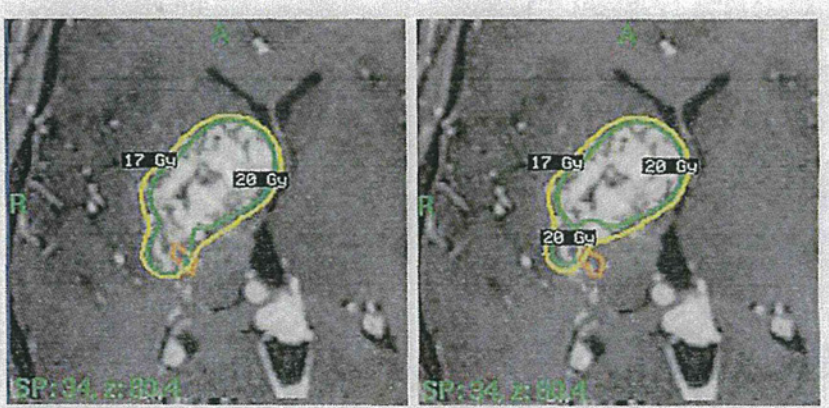

Fig. 1. Radiosurgical dosimetry of 23-year-old woman with ruptured arteriovenous malformation in the right basal ganglia. Dose delivered to the corticospinal tract before referring to tractography (a) was intentionally reduced after its integration (b).

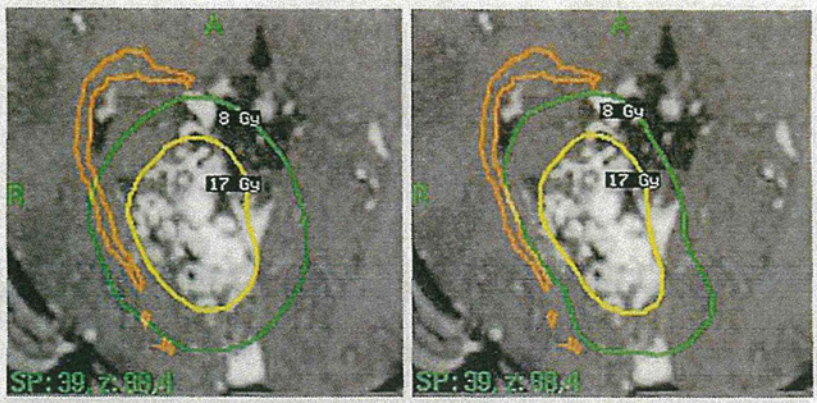

Fig. 2. Radiosurgical dosimetry of 33-year-old woman with unruptured arteriovenous malformation in the right occipital lobe. Dose delivered to the optic radiation before referring to tractography (a) was intentionally reduced after its integration (b).

follow-up at 45 months. This was the only patient who developed permanent morbidity after the prospective integration of tractography. Another patient exhibited mild transient hemiparesis 12 months after treatment prospectively integrating pyramidal tractography but fully recovered after administration of oral corticosteroid agents. Frequency of pre-existing epileptic attacks increased in 3 patients, and new onset of convulsive seizure was observed in 1 patient after radiosurgery. Nidus obliteration was confirmed by magnetic resonance imaging or angiography in 42 patients (29%) until last follow-up. Posttreatment hemorrhage was observed in 2 patients during 319 patient-years. Neither of them exhibited radiation-induced neuropathy before their subsequent hemorrhage. The other patients had no complications throughout the follow-up period.

DISCUSSION

By integrating diffusion tensor tractography of the brain white matter to radiosurgery, permanent and transient morbidity could be reliably prevented in our patients with brain arteriovenous malformations. Although many results of utilizing diffusion tensor–based tractography for diagnostic purposes have been reported (17), its integration into treatment planning of radiosurgery is our original technique and has not been performed at any other institute. Therefore, though this is a retrospective case series, reporting our results would be the most appropriate means to evaluate its efficacy.

Although there are a variety of white matter fiber tracts, we considered that the pyramidal tract would be the most important tract in preventing morbidity of radiosurgery because its injury causes motor paresis and leads to decline of activities of daily living (18, 19). At the same time, the pyramidal tract was practically the easiest one to draw from the technical point of view (17). The optic radiation and the arcuate fasciculus would be next important and are more difficult to draw (20, 21). Injury of the optic radiation causes visual disturbance. Verbal function requires participation of a distributed neural system in the dominant hemisphere, and we integrated the arcuate fasciculus tractography to preserve this function as much as practically possible. For the time being, we are introducing the above three tracts, considering them as critical white matter structures to be preserved. Technical difficulty is also a consideration, as mentioned above. Confirming above three tracts along with anatomically identifiable critical structures of the brain would be sufficient to prevent major disabling morbidity.

Integration of tractography into intraoperative navigation was also developed at our institute (13). However, it contains risks of inevitable brain shift caused by craniotomy or tumor removal, thus leading to poorer accuracy. On the other hand, such a shift does not occur in the setting of integration of tractography into radiosurgery. Therefore, we believe this would be the most suitable clinical application of diffusion tensor tractography in treating brain disorders.

Our study has several potential limitations. Our follow-up period was not long enough to evaluate late adverse events after radiosurgery (6), although it would be appropriate to observe early radiation injury that usually occurs 6 months to 2 years after radiosurgery (2, 6). Longer follow-up would be necessary to investigate whether delayed radiation-induced neuropathy does not affect our result.

Furthermore, the obliteration rate in this study group was low, probably because the median follow-up period of 23 months was shorter than that usually necessary for nidus obliteration, which is 3–5 years (22). One concern is that obliteration on imaging or subsequent prevention of future hemorrhage, which is the therapeutic goal of radiosurgery for arteriovenous malformations, can be compromised by modification of treatment planning by referring to tractography. Therefore, we need to prove, by longer follow-up, that this technique can provide morbidity prevention without lowering the obliteration rate.

Another limitation of tractography is its reliability. There is no guarantee that fibers do not exist where the tracts is not drawn (17, 23). However, tractography has been

proven to reflect anatomic pyramidal tract functioning in intraoperative fiber stimulation analysis (24). Therefore, as indicated in this study, irradiation while paying attention to firmly depicted fibers could sufficiently prevent morbidity, and practically this is the best and the only way to prevent morbidity.

The fact that the rate of tractography integration was higher in the last 2 years suggests the feasibility and usefulness of the procedure. We hope our technique will also be applied to future treatment planning software so that even physicians who are unfamiliar with complicated imaging processing can utilize our methodology (10).

REFERENCES

1. Leksell L. Cerebral radiosurgery. I. Gammathalamotomy in two cases of intractable pain. *Acta Chir Scand* 1968;134: 585–595.
2. Maruyama K, Kawahara N, Shin M, *et al.* The risk of hemorrhage after radiosurgery for cerebral arteriovenous malformations. *N Engl J Med* 2005;352:146–153.
3. Maruyama K, Kondziolka D, Niranjan A, *et al.* Stereotactic radiosurgery for brainstem arteriovenous malformations: Factors affecting outcome. *J Neurosurg* 2004;100:407–413.
4. Maruyama K, Shin M, Kurita H, *et al.* Proposed treatment strategy for cavernous sinus meningiomas: A prospective study. *Neurosurgery* 2004;55:1068–1075.
5. Andrade-Souza YM, Zadeh G, Scora D, *et al.* Radiosurgery for basal ganglia, internal capsule, and thalamus arteriovenous malformation: Clinical outcome. *Neurosurgery* 2005;56:56–64.
6. Flickinger JC, Kondziolka D, Lunsford LD, *et al.* A multiinstitutional analysis of complication outcomes after arteriovenous malformation radiosurgery. *Int J Radiat Oncol Biol Phys* 1999;44:67–74.
7. Pollock BE, Gorman DA, Brown PD. Radiosurgery for arteriovenous malformations of the basal ganglia, thalamus, and brainstem. *J Neurosurg* 2004;100:210–214.
8. Sasaki T, Kurita H, Saito I, *et al.* Arteriovenous malformations in the basal ganglia and thalamus: Management and results in 101 cases. *J Neurosurg* 1998;88:285–292.
9. Maruyama K, Kamada K, Ota T, *et al.* Tolerance of pyramidal tract to gamma knife radiosurgery based on diffusion-tensor tractography. *Int J Radiat Oncol Biol Phys* 2008;70:1330–1335.
10. Maruyama K, Kamada K, Shin M, *et al.* Integration of three-dimensional corticospinal tractography into treatment planning for gamma knife surgery. *J Neurosurg* 2005;102:673–677.
11. Maruyama K, Kamada K, Shin M, *et al.* Optic radiation tractography integrated into simulated treatment planning for Gamma Knife surgery. *J Neurosurg* 2007;107:721–726.
12. Masutani Y, Aoki S, Abe O, *et al.* MR diffusion tensor imaging: Recent advance and new techniques for diffusion tensor visualization. *Eur J Radiol* 2003;46:53–66.
13. Kamada K, Todo T, Masutani Y, *et al.* Combined use of tractography-integrated functional neuronavigation and direct fiber stimulation. *J Neurosurg* 2005;102:664–672.
14. Spetzler RF, Martin NA. A proposed grading system for arteriovenous malformations. *J Neurosurg* 1986;65:476–483.
15. Maruyama K, Koga T, Kamada K, *et al.* Arcuate fasciculus tractography integrated into Gamma Knife surgery. *J Neurosurg* 2009;111:520–526.
16. Koga T, Maruyama K, Igaki H, *et al.* The value of image coregistration during stereotactic radiosurgery. *Acta Neurochir (Wien)* 2009;151:465–471.
17. Yamada K, Sakai K, Akazawa K, *et al.* MR tractography: A review of its clinical applications. *Magn Reson Med Sci* 2009;8:165–174.
18. Andrade-Souza YM, Ramani M, Scora D, *et al.* Radiosurgical treatment for rolandic arteriovenous malformations. *J Neurosurg* 2006;105:689–697.
19. Hadjipanayis CG, Levy EI, Niranjan A, *et al.* Stereotactic radiosurgery for motor cortex region arteriovenous malformations. *Neurosurgery* 2001;48:70–76.
20. Yamamoto A, Miki Y, Urayama S, *et al.* Diffusion tensor fiber tractography of the optic radiation: Analysis with 6-, 12-, 40-, and 81-directional motion-probing gradients, a preliminary study. *AJNR Am J Neuroradiol* 2007;28:92–96.
21. Catani M, Jones DK, ffytche DH. Perisylvian language networks of the human brain. *Ann Neurol* 2005;57:8–16.
22. Shin M, Maruyama K, Kurita H, *et al.* Analysis of nidus obliteration rates after gamma knife surgery for arteriovenous malformations based on long-term follow-up data: The University of Tokyo experience. *J Neurosurg* 2004;101:18–24.
23. Holodny AI, Watts R, Korneinko VN, *et al.* Diffusion tensor tractography of the motor white matter tracts in man: Current controversies and future directions. *Ann N Y Acad Sci* 2005; 1064:88–97.
24. Kamada K, Todo T, Ota T, *et al.* The motor-evoked potential threshold evaluated by tractography and electrical stimulation. *J Neurosurg* 2009;111:785–795.

Neurol Med Chir (Tokyo) 52, 119 ~ 141, 2012

The Guidelines for Awake Craniotomy

Guidelines Committee of The Japan Awake Surgery Conference

Preface

Cortical mapping by awake craniotomy has become frequently used worldwide as part of the treatment strategy for brain lesions located near language areas. However, no systematic guidelines have been established for this surgery. The Japan Awake Surgery Conference has now created guidelines for awake craniotomy for brain lesions near language areas.

The Japan Awake Surgery Conference was established in 2002 for the purpose of continuing research into neurocognitive functions as well as establishing and promoting safe methods of awake craniotomy. The 4th annual meeting of this conference decided to establish guidelines for awake craniotomy and organized a guidelines committee. Members specializing in the fields of neurosurgery, neurology, and anesthesiology took part in discussions, a systematic review was carried out, and the guidelines committee attempted to create guidelines in compliance with evidence-based medicine methods as far as possible. However, the absence of randomized control trials of awake craniotomy forced the guidelines committee to use "de facto standards" to create the guidelines.

The guidelines consist of three parts: 1) Surgical maneuvers for awake craniotomy, 2) Anesthetic management for awake craniotomy, and 3) Language assessment during awake craniotomy. The guidelines are not intended to override the methods of experienced practitioners, and are not intended to exclude methods other than those included. We hope that these guidelines will improve the safety of awake surgeries and promote the development of the neuroscience of neurocognitive function.

President of The Japan Awake Surgery Conference
Takamasa KAYAMA, MD

I. SURGICAL MANEUVERS FOR AWAKE CRANIOTOMY

Indications

1. Age

[Recommendation]

While there is no specific upper age limit, an anesthesiologist, surgeon, and speech therapist should consider the condition of each patient carefully. Surgeons with little experience of awake craniotomy should try to perform awake surgery only in patients aged from 15 to 65 years.

[Commentary]

Awake surgery is usually performed in patients aged from 15 to 65 years. However, patients indicated for such surgery are not only specified by age. If the required tasks can be handled correctly, awake surgery can be performed in persons younger than 15 years and older than 65 years. Patients can undergo such surgery at any age if they are considered to be suitable candidates after other factors have been assessed. The cortex is difficult to excite by electrical stimulation in children aged 7 years or younger, so they do not fulfill the criteria for cortical electrical stimulation.[1] Patients older than 70 years, who may develop delirium or marked emergent increase in blood pressure, require especial attention.

Reference

1) Berger MS, Ojemann GA, Lettich E: Neurophysiological monitoring during astrocytoma surgery. *Neurosurg Clin N Am* 1: 65-80, 1990

These guidelines are approved by The Japan Neurosurgical Society. The part on anesthetic management is approved by the Japan Society of Anesthesiology and the part on language assessment during awake craniotomy is approved by the Neuropsychology Association of Japan.

Correspondence to: Takamasa Kayama, MD, Department of Neurosurgery, Yamagata University Faculty of Medicine, 2-2-2 Iida-nishi, Yamagata, Yamagata 990-9585, Japan.
Phone: +81-23-628-5349; FAX: +81-23-628-5351.

2. Diseases

[Recommendation]

In principle, the indication is for intramedullary diseases that can be treated surgically.

[Commentary]

Epilepsy without macroscopic demarcation between the normal brain tissue and the lesion, gliomatosis with indistinct borders, and cavernous hemangiomas that can only be reached through normal brain regions are typical indications.[1] Metastatic brain tumors are sometimes an indication. Extramedullary tumors such as meningioma are a less common indication, depending on the case.[2] For example, extramedullary tumor corresponding to brain disease with extended motor nerve involvement may be an indication.

References

1) Muragaki Y, Maruyama T, Iseki H, Takakura K, Hori T: [Functional brain mapping and electrophysiological monitoring during awake craniotomy for intraaxial brain lesions]. *No Shinkei Geka Journal* 17: 38–47, 2008 (Japanese)
2) Shinoura N, Yoshida M, Yamada R, Tabei Y, Saito K, Suzuki Y, Takayama Y, Yagi K: Awake surgery with continuous motor testing for resection of brain tumors in the primary motor area. *J Clin Neurosci* 16: 188–194, 2009

3. Sites

[Recommendation]

Areas indicated for awake surgery are locations where surgical procedures may lead to worsening of neurological symptoms, but can be assessed by the performance of intraoperative tasks.

[Commentary]

Lesions in and around the anatomical language areas, lesions in the lateral parietal lobe of the dominant hemisphere (mainly including the angular gyrus), lesions adjacent to the arcuate fibers (superior longitudinal fasciculus), lesions adjacent to the motor cortex, etc.

Awake surgery is indicated for lesions affecting the triangular and opercular regions of the posterior part of the inferior frontal gyrus (Brodmann's areas 44 and 45) or the inferior part of the precentral gyrus with respect to the language motor center, as well as lesions in the posterior half of the superior, middle, and inferior temporal gyri of the temporal lobe (areas 41, 42, 22, and 37) or the supramarginal and angular gyri of the parietal lobe (areas 40 and 39) with respect to the sensory language center. Awake surgery is also indicated for lesions adjacent to the arcuate fibers (superior longitudinal fasciculus) that appear to connect the motor and sensory language areas. The hippocampus is located deep inside the temporal lobe, and is associated with verbal memory, and includes the insular gyri.[1] If a lesion is located near any of the above sites in the dominant hemisphere or if the lesion cannot be confirmed to affect the nondominant hemisphere, identify the functional areas by stimulation.

Reference

1) Muragaki Y, Maruyama T, Iseki H, Takakura K, Hori T: [Functional brain mapping and electrophysiological monitoring during awake craniotomy for intraaxial brain lesions]. *No Shinkei Geka Journal* 17: 38–47, 2008 (Japanese)

4. Other indications such as neurological symptoms

[Recommendation and commentary]

The patient has to participate in awake surgery, so the patient, assessors, surgeons, and anesthesiologists must all fully understand the meaning of aggressive resection and possible complications, and be able to recognize whether or not the patient can tolerate awake anesthesia.

If patients have already developed moderate or severe symptoms, mapping and monitoring are difficult to perform. For example, patients with impairment of language functions, such as understanding, reading, repetition, and object naming, are not suitable for awake surgery. Among patients who cannot speak fluently but have no disorders of understanding, those with minor naming disorders and decreased word enumeration are candidates, although severe disorders may develop during surgery.[1]

Patients with serious intracranial hypertension and those with serious systemic complications are not suitable.

Reference

1) Berger MS, Ojemann GA, Lettich E: Neurophysiological monitoring during astrocytoma surgery. *Neurosurg Clin N Am* 1: 65–80, 1990

5. Determination of the dominant hemisphere

[Recommendation]

Performance of a provocation test (Wada test) by cerebral angiography is desirable. If determination of the dominant hemisphere is done by noninvasive tests such as functional magnetic resonance imaging (fMRI), the therapeutic strategy should be defined after considering the possibility of pseudolocalization.

[Commentary]

Various advanced procedures such as fMRI, mag-

netoencephalography (MEG), and near infrared spectroscopy (NIRS) have been developed as functional tests. These procedures are noninvasive and have made substantial contributions to neuroscience and neurology. However, for decision-making about surgical resection, the "gold standard," which is the most reliable procedure available (the procedure used to define the "correct answer" as the standard for comparison with new procedures), should be used. The gold standards for identification of the dominant hemisphere, functional areas, and neuronal functions are the provocation test (Wada test), that involves infusion of anesthetic during cerebral angiography, identification of functional sites by electrical stimulation, and neurological testing, respectively. Although the anesthetic for the Wada test was amobarbital in the original proposal, propofol is primarily used these days because amobarbital is not currently marketed in Japan.[3] These "gold standard" procedures should be used despite being more invasive because, if less invasive but less reliable procedures are used and an incorrect result is obtained, the invasiveness of surgery may become greater than necessary. Determination of the dominant hemisphere in patients with tumors causing compression based on fMRI may have left-right errors (pseudolocalization) in 14%.[4] The surgical strategy largely depends on whether or not a lesion affects the dominant hemisphere and incorrect information naturally increases the risk, so performing the Wada test (the gold standard preoperative procedure) is considered to be necessary. Although textbooks state that 99% of right-handed persons are left hemisphere dominant, a meta-analysis of 734 patients undergoing the Wada test (including 121 of our patients)[2] revealed that the dominant hemisphere for right-handed persons was the left hemisphere in 88%, the right in 5%, and both in 7%.[1] The dominant hemisphere determined by electrical stimulation is the left hemisphere in 91% and the right in 9%. Thus, around 90% of right-handed persons are left hemisphere dominant and around 10% are right hemisphere dominant, which is not a low prevalence, suggesting that careful attention should be paid during surgery to lesions in functional areas of the dominant hemisphere. The results of the Wada test in left-handed people have shown that the left dominant:right dominant ratio ranges from 1:1 to 3:1, with a slightly higher rate of left dominance.

In recent years, the increasing accuracy of noninvasive procedures such as fMRI, MEG, and NIRS has provided us with more and more knowledge. In addition, when a gradual transition from invasive to noninvasive procedures occurs because of the risk of complications of cerebral angiography, including the Wada test, the risk of pseudolocalization should be accepted. Feedback with respect to comparison of the results of the Wada test and those of mapping by electrical stimulation is needed.

References

1) Ishikawa T, Muragaki Y, Maruyama T, Ono Y, Abe K, Tanaka M, Amano K, Inoue T, Kubo O, Iseki H, Hori T, Sakai K: [Efficacy of the determination of the dominant hemisphere by Wada test and functional MRI for tumors around language areas]. Presented at the 65th Annual Meeting of the Japan Neurosurgical Society; October 18–20, 2006; Kyoto (Japanese)
2) Medina LS, Bernal B, Ruiz J: Role of functional MR in determining language dominance in epilepsy and nonepilepsy populations: a Bayesian analysis. *Radiology* 242: 94–100, 2007
3) Takayama M, Miyamato S, Ikeda A, Mikuni N, Takahashi JB, Usui K, Satow T, Yamamoto J, Matsuhashi M, Matsumoto R, Nagamine T, Shibasaki H, Hashimoto N: Intracarotid propofol test for speech and memory dominance in man. *Neurology* 63: 510–515, 2004
4) Ulmer JL, Hacein-Bey L, Mathews VP, Mueller WM, DeYoe EA, Prost RW, Meyer GA, Krouwer HG, Schmainda KM: Lesion-induced pseudo-dominance at functional magnetic resonance imaging: implications for preoperative assessments. *Neurosurgery* 55: 569–581, 2004

Methods

1. Preoperative treatment

1-1. Status and details of simulation

[Recommendation]

The tasks that will be performed during surgery should be preoperatively rehearsed in the ward. Simulation of the surgical posture, equipment set-up, and role sharing, as well as rehearsal of the tasks for the patient, surgeons, anesthesiologists, and other surgical staff (such as nurses) should also be performed in the operating room.

[Commentary]

For successful intraoperative mapping with awake anesthesia, it is important to reduce the patient's anxiety as much as possible by maintaining a comfortable environment during surgery. Bring the patient to the operating room on the day before surgery, and take enough time to explain what will be done on the next day (including the posture that the patient will be placed in by the surgeon, anesthesiologists, and nurses). Then have the patient actually adopt that posture. If possible, show the patient a video of surgery on previous patients for better understanding. If functional language mapping is performed, conduct higher function exami-

nation before surgery, perform the tasks that will done during surgery in the ward in advance, and select intraoperative tasks, for example, by showing the patient pictures or photographs of common objects used in object naming and selecting some that the patient can answer correctly. If there has been a long interval between examination and surgery in a patient with progressive symptoms due to a tumor adjacent to the language areas, the tasks should be selected immediately before surgery.

1-2. Monitoring of anticonvulsants

[Recommendation]

In patients who are scheduled to undergo awake surgery, it is desirable to initiate the administration of anticonvulsants in advance and maintain effective blood concentrations if enough time is available. Phenytoin can be administered and the concentration increased to the upper limit of the effective range (target level 20 mg/dl) by the day before surgery.

[Commentary]

Even if an effective blood concentration of an anticonvulsant has been maintained since before surgery, there is some risk of convulsions during awake surgery (as described below). Therefore, sufficient preoperative antiepileptic drug saturation is desirable to prevent intraoperative convulsions and for easy drug loading after the onset of convulsions. Regarding the selection of drugs, phenytoin is recommended, since intravenous administration can be performed immediately before or during surgery when oral administration is not possible, rapid saturation is easy, a steady-state blood concentration can be obtained after a relatively short time (4–5 days), and regulation of the blood concentration is easy.

The bioavailability of phenytoin is high (98%) and there is little difference between systemic absorption after intravenous and oral administration. If there are 3 or more days before surgery, it is desirable to achieve the target blood concentration by oral administration to reduce patient discomfort. If rapid saturation immediately before surgery is selected, the target blood concentration can be obtained promptly by intravenous administration of phenytoin.

Especially for patients with tumors located near the motor cortex, after obtaining an adequate preoperative blood concentration of phenytoin, the blood level should be monitored every 2 hours during surgery. If the concentration is low, intravenous administration of 250 mg of phenytoin should be given to raise the concentration to the normal upper limit (this dose increases the blood level by approximately 6 mg/dl in a patient weighing 60 kg), or 100–200 mg of phenytoin should be given every 4 hours during surgery (this dose will increase the blood level by approximately 2.4–4.7 mg/dl in a patient weighing 60 kg).

Sixteen (16%) of the 100 patients who underwent awake surgery at Tokyo Women's Medical University from 2004 to the present developed seizures under awake conditions, whereas 48 (48%) of these 100 patients had a history of seizures before surgery. Twelve (24.5%) of the 49 patients with tumors near the motor cortex developed seizures during awake surgery and this rate was higher than at other sites. Occurrence of seizures during awake surgery is defined as clinically obvious convulsions and does not include patients who only have afterdischarges.

Among the 80% or more of our 100 patients who had received preoperative antiepileptic drug therapy, patients with lesions near the motor cortex and a preoperative blood level within or above the effective range accounted for 70% of patients both with and without intraoperative convulsions, although the blood level was not measured in all patients. Thus, even if the blood level of an antiepileptic drug is within the effective concentration range, there is no improvement of the preventative effect against intraoperative seizures, which is more likely to depend on the conditions of electrical stimulation.

Preoperative phenytoin loading is not performed at Tokyo Women's Medical University, so its efficacy has not been demonstrated there. Therefore, the frequency of intraoperative convulsions in patients with brain lesions at each site should be compared with that determined at institutions where rapid preoperative phenytoin saturation is performed to assess the usefulness of this procedure. It may also be necessary to assess the conditions employed for electrical stimulation, especially for the motor cortex, as well as the use of rapid anticonvulsant saturation.

[Saturation][1,2]

Initial loading dose [mg]: target blood concentration [mg/dl] × volume of distribution Vd [l/kg] × body weight [kg] = 20 × 0.7 × body weight [kg]..(a)

Additional loading dose [mg]: {target blood concentration − measured value [mg/dl]} × volume of distribution Vd [l/kg] × body weight [kg] = {20 − measured value) × 0.7 × body weight [kg].....(b)

Where target blood concentration is 20 mg/dl, and Vd is specific value for each drug: phenytoin 0.6–0.8 (approximately 0.7) l/kg.

For example, in a patient weighing 60 kg, the initial loading dose calculated using (a) is 840 mg, which is administered as three divided doses every 2

to 4 hours. This will avoid cardiovascular adverse reactions such as hypotension, bradycardia, and arrhythmia, as well as gastrointestinal symptoms. After 12 to 24 hours of administration at the above dose, initiate therapy at the usual maintenance dose (200–400 mg/day). Measure the blood concentration 2 to 3 days after finishing the initial loading dose for oral administration, and at 24 hours after or immediately before surgery when rapid saturation has been achieved by intravenous administration, and calculate the additional loading dose using (b).

The saturation period for phenytoin should be within the range of 3 to 5 days to avoid the development of adverse reactions when the blood level is maintained at the upper limit of the effective concentration range for too long (1 week or more) before surgery. There have been many reports about phenytoin-induced skin disorders such as disseminated erythematous papules after approximately 2 weeks and serious drug-induced hypersensitivity syndrome after 2 to 6 weeks in most cases.[3]

Because the protein-binding rate of phenytoin is high (90–95%), even if the blood level of the drug is within the effective range in patients who have a low serum albumin concentration, the concentration of free drug (not bound to albumin) will be increased and measured values may not reflect the actual levels. If the serum albumin is 3 g/dl or lower, free phenytoin should be simultaneously measured or the effective phenytoin concentration estimated using the following formula for correction: Measured phenytoin level/{(0.2 × albumin level) + 0.1} .....(c)

Where target range for free phenytoin is 2 to 2.5 mg/dl.

References

1) Lacy CF, Armstrong LL, Goldman MP, Lance LL: *Lexi-Comp's Drug Information Handbook, 13th ed.* Ohio, Lexi-Comp Inc, 2005, pp 1195–1199
2) Ogata H, Masuhara K, Matsumoto Y: [*Clinical Pharmacokinetics*]. Osaka, Maruzen, 2001, 181 pp (Japanese)
3) Shiohara T, Miyachi Y, Takigawa M (eds): [*Dermatology Practice 19; Master Drug Eruption*]. Tokyo, Bunkodo, 2006, 301 pp (Japanese)

2. Various intraoperative methods

2-1. Sites and methods of local scalp anesthesia

[Recommendation]

For local anesthesia of the scalp, it is common to use long-acting local anesthetics in combination with invasive anesthesia and nerve blocks.

[Commentary]

Analgesia by local anesthesia is often performed by the combination of infiltration with local anesthetic and nerve blocks. At some institutions, anesthesia is performed only by local injection or only by nerve block. Long-acting local anesthetics such as ropivacaine and bupivacaine are often used and these are combined with lidocaine at some institutions.[3] Supraorbital nerve block is used if the skin incision is primarily located in the frontal region, whereas auriculotemporal nerve block is used for an incision in the temporal region. Greater or lesser occipital nerve blocks can be added to these blocks. If head fixation is used, an anesthetic is administered at the sites of the pins in addition to the skin incision sites. Sufficient anesthetic should be provided at the pin sites because many patients complain of pain at these sites during emergence.

Preoperative simulation of temporary pseudo-emergence can be performed after fixing the head in a specific posture before the initiation of surgery, to confirm whether tasks can be performed or whether there are any problems with the removal and reinsertion of a laryngeal mask.[1,2]

References

1) Fukaya C, Katayama Y: [Intraoperative wake up procedure using propofol total intravenous anesthesia and laryngeal mask]. *No Shinkei Geka Journal* 8: 332–337, 1999 (Japanese)
2) Fukaya C, Katayama Y, Yoshino A, Kobayashi K, Kasai M, Yamamoto T: Intraoperative wake-up procedure with propofol and laryngeal mask for optimal excision of brain tumour in eloquent areas. *J Clin Neurosci* 8: 253–255, 2001
3) Sato K, Kawamata M, Nagata O, Kawaguchi M, Morimoto Y, Kato M, Sakabe T: [Present state of anesthetic management for awake craniotomy in Japan]. *Masui* 57: 492–496, 2008 (Japanese)

2-2. Head fixation and posture setting

[Recommendation]

Successful awake functional brain mapping/monitoring depends on whether the patient's cooperation can be maintained for a long time. Therefore, head fixation and posture setting are important to keep the patient in a comfortable position for a long period.

Although there is no definitive method of head fixation and posture setting, continuous feedback is essential about whether functional brain mapping/monitoring is successful or not, and whether or not the patient can comfortably cooperate with surgery and functional brain mapping/monitoring, and the surgeon should continue to assess whether the selected method is correct or not.

The basic procedure is as follows:

i) Preoperative explanation: It is important to create an image of surgery for the patient and family. If

this is not done, the patient will not understand what to do and how to cooperate, and will be uneasy during the surgery. The preoperative explanation should include basic issues related to brain functional differentiation, association of the extent of tumor invasion with functional areas, neurosurgical procedures, and functional brain mapping/monitoring procedures, and be illustrated with pictures, slides, and videos. Also, bring the patient to the actual operating room before surgery, perform head fixation and posture setting, and allow enough time to perform surgical simulation that includes meeting with the surgeons and nurses.

ii) Head fixation: Whether complete restriction of movement of the head by pin fixation or to allow movement of the head by not performing fixation is better has not been decided. The purpose of surgery is to safely and reliably resect the tumor, and the method should be established at each institution that both maintains patient comfort and allows surgery to achieve its purpose.

iii) Posture setting: To perform functional mapping of motor and sensory areas including functional language mapping, craniotomy must extend to sites that include normal brain tissue as well as the tumor. A posture that allows the performance of wide frontal-temporal-parietal craniotomy is generally used. For posture setting, given that the body weight is supported by various parts of the body, individual differences with regard to a comfortable posture and how painful maintaining the same posture for a long time can be for patients must be fully understood. Setting a posture that is only tolerable for a short time and attempting to maintain it for a long time leads to pain at unexpected sites. How many times the posture can be changed during surgery and the patient's desired temperature (hot or cold) must also be confirmed.

[Commentary on approach without head fixation]
Posture setting

What surprised us most when we visited the institution of Berger et al., who are pioneers in the use of this method for maximum resection of gliomas, is that Dr. Berger himself took time to carefully set each patient's posture with pads that were tailor-made for size, shape, and thickness. Their stock of prepared pads and linen was much larger than ours. Awake surgery provides us with a good opportunity to realize how inadequate our previous posture setting is for general anesthesia. The following posture setting and head fixation procedures are basically according to the method of Berger et al.[1-3]

Preparation on the day before surgery: Bring the patient to the actual operating room on the day before surgery, and take enough time to explain what will be done on the next day, including posture setting. It is important for the patient to meet the surgeons, assistants, anesthesiologists, and nurses. At that time, detailed explanation of the patient's pathological condition, and explanation using videos about tumor resection in combination with awake functional brain mapping/monitoring should be provided to the patient (permission for the use of videos should be obtained because they contain personal information). It is as important for the patient to have an understanding of the surgery as it is for the surgeons to develop an image of the procedure.

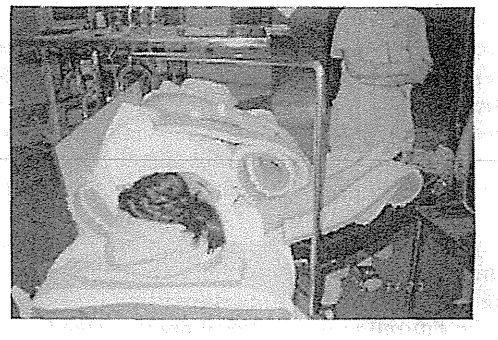

Fig. 1 Posture setting in the Department of Neurosurgery of Tohoku University.

To perform functional mapping of motor and sensory areas, including functional language mapping, craniotomy needs to expose normal brain tissue as well as the tumor. In general, to allow for wide frontal-temporal-parietal craniotomy, the head is tilted 75° to the opposite side. The next section covers whether head fixation should be performed or not. Place a large pad supporting the whole body from the shoulder to the waist to avoid torsion of the shoulders and head. To improve venous return, slightly raise the upper part of the body. Find the most comfortable positions for both the upper and lower extremities, and be careful not to overload any part of the body. It is desirable to fill little empty spaces with small pads. During posture setting, maintain an environment similar to that during the actual surgery as far as possible, continue conversation, and take time to check for the presence or absence of pain and to be careful not to have any body part unsupported (Fig. 1).

To perform mapping, you need to have a clear space in front of the patient's eyes and to have enough space to place a portable computer within the vision, which is used for object naming in functional language mapping. At our hospital, this space is created with L-shaped bars and infusion stands